THE GEOLOGICAL SOCIETY OF AMERICA®

Hydrogen incorporation and retention in metamorphic olivine during subduction: Implications for the deep water cycle

Elias D. Kempf* and Jörg Hermann
Institute of Geological Sciences, University of Bern, Baltzerstrasse 3, 3012 Bern, Switzerland

ABSTRACT

Incorporation of hydrogen into metamorphic olivine during dehydration reactions in the subducting oceanic lithosphere provides a mechanism to replenish the deep mantle with water. Fourier transform infrared spectroscopy of metamorphic olivines formed at 2.5 GPa and 550 °C through the reaction antigorite + brucite = olivine + chlorite + water shows water contents between 100 and 140 ppm H_2O associated exclusively with silicon vacancies, similar to the highest values found in peridotite xenoliths. Brucite involvement in the olivine-forming reaction ensures H_2O saturation and a low Si activity, favoring hydrogen incorporation into Si vacancies. The mapped water distribution in olivine is consistent with growth zoning and there is no evidence of water gain or loss. Thus, even for metamorphic timescales of several million years at 550 °C, no ionic diffusion modification is observed, in agreement with recent experimental findings. Metamorphic olivines formed by this dehydration reaction may contribute considerable amounts of water to the deep water cycle. Additionally, olivine with abundant H in Si vacancies are expected to be rheologically weaker than anyhdrous mantle olivine, and might provide a weak interface between slabs and mantle wedges in subduction zones at conditions beyond the stability of hydrous phases.

INTRODUCTION

Hydrous minerals in ultramafic rocks are considered the main carriers of water (in the form of structural OH) from the surface to Earth's interior along subduction zones (Schmidt and Poli, 1998). Serpentinization of mantle peridotite at mid-ocean ridges produces hydrous phases such as serpentine and brucite. Water is released by the breakdown of these phases during prograde subduction metamorphism, and resulting fluids are recycled back to Earth's surface via hydrothermal activity or arc magmatism. A key question in this deep water cycle is how, and how much, water is transferred from the hydrous phases of serpentine and brucite to nominally anhydrous minerals (NAMs), such as olivine and pyroxene, during dehydration reactions. Once OH is incorporated into NAMs, it can be carried to greater depth in subduction zones. This represents a key process in how water is transported beyond sub-arc depth to replenish the deeper mantle (Peacock, 1990; Hirschmann and Kohlstedt, 2012). As the viscosity of olivine decreases with OH incorporation, particularly when it replaces silicon (Mackwell et al., 1985; Mei and Kohlstedt, 2000), the rheology at the interface of the subducted crust with the mantle wedge will also be affected (Faul et al., 2016). To answer these key questions, it is important to know how much, and in which site, OH is incorporated into metamorphic olivine formed by dehydration reactions during subduction.

There have been numerous experimental studies on OH incorporation into olivine at high temperatures (typically 900–1200 °C), providing a framework to constrain the capacity to host water in the lithospheric and asthenospheric mantle (Kohlstedt et al., 1996; Férot and Bolfan-Casanova, 2012; Smyth et al., 2006). Much less is known about OH incorporation at conditions relevant for subduction-zone conditions, because experiments are impractical at the corresponding low temperatures of 450–650 °C owing to slow kinetics. There is only one recent experimental study that has shown that ~5–50 ppm (μg g^{-1}) of H_2O can be incorporated in Ti- and Fe-bearing olivine after the antigorite breakdown at 650–700 °C (Padrón-Navarta and Hermann, 2017):

$$\text{antigorite} \rightarrow \text{olivine} + \text{orthopyroxene} + \text{chlorite} + \text{water}. \quad (1)$$

No data however, are available for the first metamorphic olivine-forming reaction in subducted serpentinites:

$$\text{brucite} + \text{antigorite} \rightarrow \text{olivine} + \text{chlorite} + \text{water}. \quad (2)$$

The comparison of experimental results on OH incorporation into NAMs and natural rocks is hampered by the fact that experiments are conducted under water-saturated conditions, whereas natural mantle rocks generally are water-undersaturated. Dehydration reactions such as those encountered during prograde subduction-zone metamorphism provide a rare natural environment where water-saturated conditions prevail, facilitating the comparison of natural rocks with experiments.

In this paper, we investigate a new mechanism of OH incorporation in metamorphic olivine produced by Reaction 2 during subduction of the Zermatt-Saas serpentinite (Western Alps, Switzerland). We quantify how much water is transferred from hydrous phases to nominally anhydrous olivine. A common problem with natural samples is that there is potential diffusive hydrogen loss in olivine after its formation. Olivines in slowly exhumed mantle rocks are unlikely to preserve the original water contents (Demouchy and Mackwell, 2003), and even olivine xenocrysts in kimberlites partially lose water in timescales of hours to days (Doucet et al., 2014). Thus, particular emphasis was placed on determining the extent to which metamorphic olivine is able to retain water during exhumation of the high-pressure olivine-bearing serpentinite. We discuss the implications of the observed water contents in metamorphic olivine on the deep water cycle and the rheology at the slab interface.

METAMORPHIC OLIVINE FORMATION

The Zermatt-Saas ophiolite represents a remnant of the Jurassic Alpine Thethys oceanic lithosphere and contains a large serpentinite body, along with meta-basalts and meta-sediments (Fig. 1A). During subduction, eclogite facies conditions of 550 °C and 2.5 GPa were reached, determined from meta-gabbros, eglogites, and rodingites (Angiboust et al., 2009; Li et al., 2008). Four samples of olivine-bearing serpentinites from a recently exposed outcrop at the side of the Unterer Theodulgletscher (Lower Theodul Glacier) were investigated (Table 1; Fig. 1A). Figure 1B shows a 1–2-m-thick shear zone consisting of 50–500 μm metamorphic olivines, which form a mosaic equilibrium texture with antigorite and chlorite (Fig. 1C). Ti-clinohumite and magnetite grains are minor phases. Two samples (Ol1, Ol2) have been investigated from this shear zone. The country rock of the shear zone is a massive olivine serpentinite (sample FA), which consists of xenoblastic 1–3 cm olivine grains (Mg# = 95–96) that contain numerous inclusions of antigorite, magnetite, micron-sized

*E-mail: elias.kempf@geo.unibe.ch

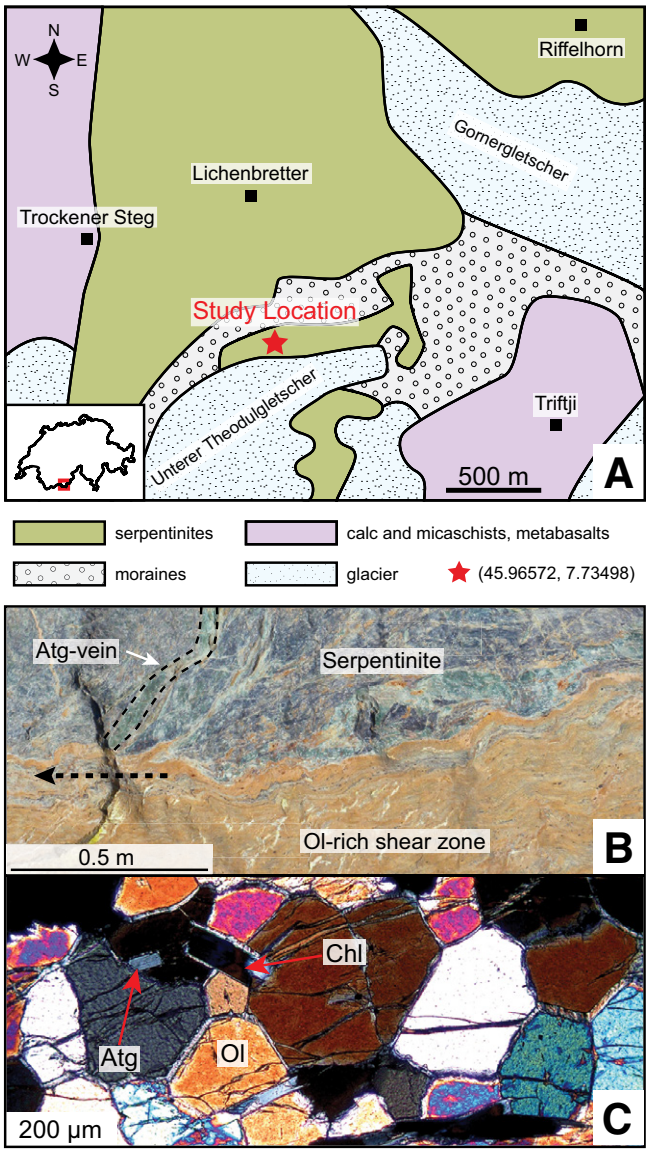

Figure 1. A: Study area in Zermatt, Switzerland, modified from the geological map of Bearth (1967). Locations of samples FA and Ol26 are within 20 m northeast of samples Ol1 and Ol2, indicated by the red star (WGS84 coordinates: latitude, longitude). B: An olivine-rich shear zone (samples Ol1, Ol2) crosscuts the high-pressure serpentinite and a prograde antigorite (Atg) vein. C: The shear zone consists mainly of idioblastic olivine (Ol) grains and trace amounts of chlorite (Chl, weak brown anomal interference colors) and antigorite (Atg). Crossed polarizer microphotograph.

chlorite blades, and lamellae of Ti-clinohumite. Olivines locally include a relic magnetite mesh texture and magnetite veins, typically formed during ocean-floor serpentinization of peridotites (Wicks and Whittaker, 1977). Occasionally, the serpentinites are crosscut by veins with centimeter-sized olivines that are partially recrystallized (sample Ol26) and associated with Ti-clinohumite, antigorite, and magnetite. The Mg# of 95–96 for the olivines is too high for a mantle origin, and the similar minor and trace element composition (including the water contents; Table DR1 in the GSA Data Repository[1]; Table 1) support the textural evidence that olivine growth is related to the metamorphic devolatilization Reaction 2. At 2.5 GPa, this reaction is divariant in the FMASH (FeO-MgO-Al_2O_3-SiO_2-H_2O) system and is crossed in a temperature interval from 490 to 540 °C for the measured local bulk composition (Fig. DR3). Hence, olivine growth occurred in the presence of brucite during prograde to peak metamorphic conditions. Additional textures of the rocks are reported in Figure DR1.

WATER INCORPORATION

Experimental studies combined with Fourier transform infrared (FTIR) spectroscopy analyses (e.g., Berry et al., 2005) and theoretical calculations (Blanchard et al., 2017) have shown that the main defects associated with the incorporation of water in olivine are (1) four hydrogens substituting for tetrahedral Si [Si], (2) two H substituting for octahedral Mg [Mg], (3) the coupled substitutions of two Mg with a trivalent cation + H [triv], and (4) the replacement of Mg by Ti charge-balanced by two H on a Si site [Ti]. The first two substitutions are dependent on the MgO and SiO_2 activity, and thus on the buffering assemblage during olivine formation, whereas the latter two mainly depend on the amount of trace elements such as Ti, Cr, Al, and Fe^{3+} in olivine. Inclusion-free, clear, idioblastic olivines from the four samples have been analyzed with polarized and unpolarized FTIR spectroscopy (see the Data Repository for methods). Unpolarized spectra display absorption bands at 3613, 3600, 3580, 3567, 3553, 3535 and 3478 cm^{-1} (Fig. 2), corresponding to Si vacancies (Berry et al., 2005; Padrón-Navarta et al., 2014; Walker et al., 2007). This is further supported by the polarized absorption along principle crystallographic axes, showing variations in absorption identical to experimental olivine with Si vacancies (Fig. DR2A). Large xenoblastic grains from the olivine vein show additional absorption bands at 3400 and 3417 cm^{-1} (Fig. DR2B) typical for Ti-clinohumite lamellae (Shen et al., 2014). Neither clinohumite point defects nor trivalent defects were observed, in agreement with very low Ti (<6 ppm), Cr (<10 ppm), and Al (<0.5 ppm) contents in the recrystallized olivine (Table DR1).

Quantification of water contents (Table 1) in olivine from the four samples was based on total absorbance from clean spectra normalized to 1 cm thickness (Fig. 2) without contamination from Ti-clinohumite lamellae or antigorite/chlorite inclusions, using the calibration factor of Bell et al. (2003). The total absorbance derived from polarized and unpolarized measurements are within standard error. All four samples display

TABLE 1. WATER CONTENTS FROM FTIR MEASUREMENTS

Sample	Description	Absorbance			Total	Polarized		Absorbance	Unpolarized	
		a ± r*	b ± r*	c ± r*		total ± r* (ppm)	n†		Total (ppm)§	n†
FA	country rock	299 ± 47	153 ± 65	128 ± 22	580 ± 83	109 ± 16	11	544	102	18
Ol1	shear zone	396 ± 80	180 ± 29	184 ± 28	760 ± 89	143 ± 17	11	645	121	15
Ol2	shear zone	390 ± 51	186 ± 14	161 ± 4	737 ± 53	139 ± 10	8	716	135	10
Ol26	olivine vein	270 ± 28	146 ± 19	150 ± 66	566 ± 75	106 ± 14	7	571	107	7

Note: Samples are stored at the Institute of Geological Sciences, Bern, Switzerland. Only spectra with distinctive overtone spectra were considered for polarized measurements.
*Standard error of averaged polarized measurements along the principle crystallographic axis.
†Number of measurements.
§Unpolarized measurements have a ± 15% error

[1]GSA Data Repository item 2018189, Table DR1, Figures DR1–DR3, and a description of method, is available online at http://www.geosociety.org/datarepository/2018/ or on request from editing@geosociety.org.

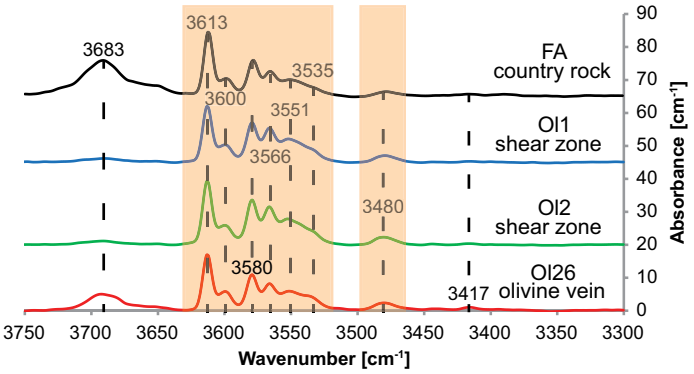

Figure 2. Averaged unpolarized spectra of olivine (scaled to 1 cm thickness) from four samples (FA, Ol1, Ol2, and Ol26; Table 1) display characteristic absorption bands related to Si vacancies (orange shaded fields). A minor absorption band around 3683 cm^{-1} represents serpentine inclusions, and the 3417 cm^{-1} band corresponds to titanian-clinohumite lamellae.

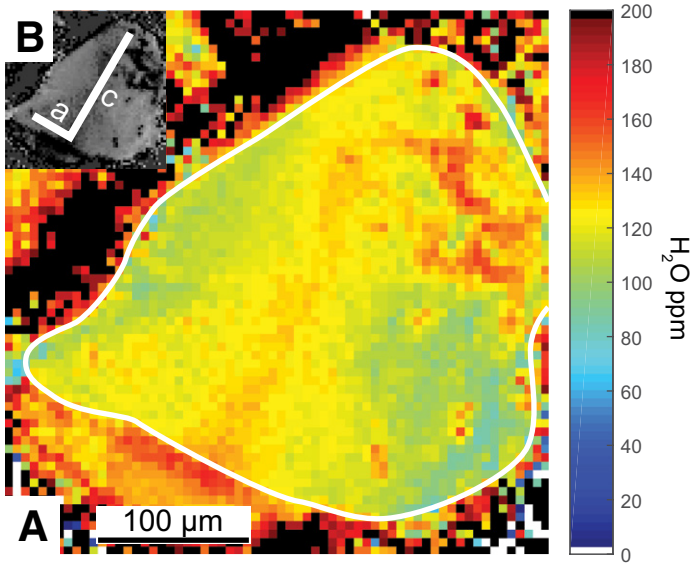

Figure 3. A: Water distribution map of an olivine grain from sample Ol1 measured with Fourier transform infrared (FTIR) spectroscopy coupled to a focal-plane-array (FPA) detector (pixel size is 5.6 × 5.6 µm). The border of the clear olivine is traced with a white line. Black pixels are associated with hydrous phases such as antigorite, whereas water-free oxides are represented by white pixels. B: Crystallographic axes determined from olivine overtones using polarized FTIR.

consistently high water contents, between 100 and 140 ppm, independent of grain size (Table 1). Water incorporation of 100 ppm H_2O into Si vacancies in olivine through Reaction 1, buffered with orthopyroxene (as is typical for natural peridotites), has been reported only at temperatures above 700 °C and pressures greater than 5 GPa (Bali et al., 2008; Mosenfelder et al., 2006; Padrón-Navarta and Hermann, 2017). Thus, the unexpected presence of exlusively Si vacancies at 2.5 GPa and 550 °C requires a new mechanism. During Reaction 2, the Si activity is more than one log unit lower than during the antigorite breakdown, Reaction 1 (Fig. DR3). The presence of brucite and olivine along the reaction in the divariant field thus imposes the low Si activity needed to form the high amount of Si vacancies and high water contents at pressure-temperature conditions relevant to subducted crust at sub-arc conditions.

WATER RETENTION

The observed [Si] defects demonstrate that OH must be incorporated in olivine while brucite is still stable; i.e., during prograde to peak metamorphic conditions. Therefore, water gain during retrogression can be excluded. The four investigated samples show, within standard error, identical water contents independent of the grain size of the analyzed olivine (Table 1; Fig. 2). This suggests that hydrogen loss by diffusion during exhumation was negligible. To further test this, the water distribution of a clear olivine grain from the shear zone was mapped with a focal-plane-array detector (Fig. 3A). The water map shows a maximum of ~130 ppm in the center of the grain, that extends toward the rim along the c-axis (Fig. 3B). Irregular zoning is present along the a-axis where H_2O contents plateau at 105 ppm at rims. This irregular zoning is interpreted as growth zoning and is unrelated to any minor zoning in major and trace elements. If ionic diffusion plays a significant role, a regular water decrease (i.e., concentric zoning) is expected, which was not observed. This implies that the H in Si vacancies was retained during exhumation. Using peak conditions of 550 °C and a conservative estimation of 5 m.y. for the exhumation time (Agard et al., 2009), we modeled diffusion profiles in olivine using different diffusivities from the literature. The down-temperature extrapolation of experimentally determined hydrogen diffusion coefficients for Mg-vacancies from Demouchy and Mackwell (2003) results in a minimum $D = 1.6 \times 10^{-18}$ m^2 s^{-1} at 550 °C. Using this diffusion coefficient in Crank's (1975) equation for one-dimensional diffusion into a semi-infinite slab shows that almost all water should have been lost during exhumation. In contrast, down-temperature extrapolation of H diffusivity in Si vacancies based on the experiments of Padrón-Navarta et al. (2014) results in a diffusion coefficient that is eight orders of magnitude lower. Modeling the diffusion at 550 °C results in negligible hydrogen loss of olivine for the maximum duration of 5 m.y.. This is the first time that slow diffusion of H associated with Si vacancies has been observed in natural samples. Additionally, our observations suggest that in these Fe- and trace element–poor olivines, no additional fast diffusion pathway is evident. Therefore, the measured water contents in olivine faithfully record the amount of water transferred from hydrous phases to olivine during subduction.

IMPLICATIONS FOR THE DEEP WATER CYCLE

The large amount of water stored in Si vacancies (Table 1) in metamorphic olivine formed by Reaction 2 is independent of any trace elements, and thus can be obtained in any subducted serpentinite containing brucite. On the basis of the averaged bulk-rock measurements of the Zermatt-Saas serpentinites of Li et al. (2004), we calculated a brucite content of 7 vol%. This amounts to 25 vol% olivine formed, on average, in the Zermatt-Saas serpentinite from Reaction 2, but in shear zones and veins, the amount of such hydrous olivine increases to 70–80 vol% (see the Data Repository section on thermodynamic modeling). The measured H_2O contents in metamorphic olivine (Table 1) is higher than in most olivines from the lithospheric mantle (Demouchy and Bolfan-Casanova, 2016), and only rare olivine in kimberlite xenoliths that originate from much higher pressures (4–6 GPa) and temperatures (>1000 °C) contain similar or higher water contents (Doucet et al., 2014). Thus, the reported H_2O contents (Table 1) incorporated into metamorphic olivine representing 30 wt% of the total rock mass at 550 °C, 2.5 GPa could represent an important mechanism to transport water into the deeper mantle by subduction. The capacity of olivine to incorporate water is significantly higher when brucite is present, imposing a low Si activity compared to olivine formed during the final breakdown of antigorite at higher temperatures, that is buffered at much higher Siactivities by orthopyroxene (Fig. DR3). Experimental investigations have shown that for sub-arc pressures of 3–5 GPa, olivine coexisting with orthopyroxene contains only 10–50 ppm of water at the antigorite breakdown (Reaction 1), and values of >150 ppm are only reached at pressures above 5 GPa and temperatures of 700–800 °C (Padrón-Navarta and Hermann, 2017). It is not yet clear

to what extent olivine formed during Reaction 2 is able to retain its water, once orthopyroxene is formed.

Our observation that water is exclusively incorporated into Si defects (Fig. 2) in olivine is also important for the rheology at the slab-mantle interface. Although the extent of water weakening is not fully resolved, it is expected that hydrogen replacement of Si will lead to a significant decrease in the viscosity of olivine (Mackwell et al., 1985; Karato et al., 1986; Tielke et al., 2017). The olivine-rich veins and shear zones in which antigorite is only a minor phase are of special interest. These rocks are more competent than serpentinites, favoring little internal deformation and recrystallization as long as chlorite and antigorite are stable. However, after their breakdown, the relationship might be reversed, where the veins and shear zones dominated by olivine with high amounts of water in Si vacancies are likely to be the weakest rock types, and thus could be the locus for nucleation of shear zones at the slab-mantle interface. Thus, olivine veins and shear zones from subducted serpentinites, such as investigated in the subducted Zermatt-Saas serpentinite, could serve as a decoupling interface between the subducted slab and the overlying mantle wedge at conditions beyond the stability of hydrous phases such as serpentine and chlorite.

ACKNOWLEDGMENTS

We thank S. Demouchy, D. Frost, and an anonymous reviewer for their constructive comments, and D. Brown for efficient editorial handling. Additionally, we thank L. Baumgartner and E. Reusser for introduction to this fascinating field area, P. Tollan for help with FTIR analyses and constructive discussions, J. Reynes for assistance with processing focal-plane-array detector maps, and D. Rubatto for helpful comments. This work was supported by the Swiss National Science Foundation project 200021_169062.

REFERENCES CITED

Agard, P., Yamato, P., Jolivet, L., and Burov, E., 2009, Exhumation of oceanic blueschists and eclogites in subduction zones: Timing and mechanisms: Earth-Science Reviews, v. 92, p. 53–79, https://doi.org/10.1016/j.earscirev.2008.11.002.

Angiboust, S., Agard, P., Jolivet, L., and Beyssac, O., 2009, The Zermatt-Saas ophiolite: The largest (60-km wide) and deepest (c. 70–80 km) continuous slice of oceanic lithosphere detached from a subduction zone?: Terra Nova, v. 21, p. 171–180, https://doi.org/10.1111/j.1365-3121.2009.00870.x.

Bali, E., Bolfan-Casanova, N., and Koga, K., 2008, Pressure and temperature dependence of H solubility in forsterite: An implication to water activity in the Earth interior: Earth and Planetary Science Letters, v. 268, p. 354–363, https://doi.org/10.1016/j.epsl.2008.01.035.

Bearth, P., 1967, Die Ophiolithe der Zone von Zermatt-Saas Fee: Bern, Kuemmerly & Frey AG, Beitr. Geo. Karte d. Schweiz, Neue Folge, 132, scale 1:25'000.

Bell, D.R., Rossman, G.R., Maldener, J., Endisch, D., and Rauch, F., 2003, Hydroxide in olivine: A quantitative determination of the absolute amount and calibration of the IR spectrum: Journal of Geophysical Research: Solid Earth, v. 108, p. 2015–2113, https://doi.org/10.1029/2001JB000679.

Berry, A.J., Hermann, J., O'Neill, H.S., and Foran, G.J., 2005, Fingerprinting the water site in mantle olivine: Geology, v. 33, p. 869–872, https://doi.org/10.1130/G21759.1.

Blanchard, M., Ingrin, J., Balan, E., Kovács, I., and Withers, A.C., 2017, Effect of iron and trivalent cations on OH defects in olivine: The American Mineralogist, v. 102, p. 302–311, https://doi.org/10.2138/am-2017-5777.

Crank, J., 1975, The Mathematics of Diffusion: Oxford, UK, Oxford University Press, 414 p.

Demouchy, S., and Bolfan-Casanova, N., 2016, Distribution and transport of hydrogen in the lithospheric mantle: A review: Lithos, v. 240–243, p. 402–425, https://doi.org/10.1016/j.lithos.2015.11.012.

Demouchy, S., and Mackwell, S., 2003, Water diffusion in synthetic iron-free forsterite: Physics and Chemistry of Minerals, v. 30, p. 486–494, https://doi.org/10.1007/s00269-003-0342-2.

Doucet, L.S., Peslier, A.H., Ionov, D.A., Brandon, A.D., Golovin, A.V., Goncharov, A.G., and Ashchepkov, I.V., 2014, High water contents in the Siberian cratonic mantle linked to metasomatism: An FTIR study of Udachnaya peridotite xenoliths: Geochimica et Cosmochimica Acta, v. 137, p. 159–187, https://doi.org/10.1016/j.gca.2014.04.011.

Faul, U.H., Cline, C.J., David, E.C., Berry, A.J., and Jackson, I., 2016, Titanium-hydroxyl defect-controlled rheology of the Earth's upper mantle: Earth and Planetary Science Letters, v. 452, p. 227–237, https://doi.org/10.1016/j.epsl.2016.07.016.

Férot, A., and Bolfan-Casanova, N., 2012, Water storage capacity in olivine and pyroxene to 14GPa: Implications for the water content of the Earth's upper mantle and nature of seismic discontinuities: Earth and Planetary Science Letters, v. 349–350, p. 218–230, https://doi.org/10.1016/j.epsl.2012.06.022.

Hirschmann, M., and Kohlstedt, D., 2012, Water in Earth's mantle: Physics Today, v. 65, p. 40, https://doi.org/10.1063/PT.3.1476.

Karato, S.I., Paterson, M.S., and FitzGerald, J.D., 1986, Rheology of synthetic olivine aggregates: Influence of grain size and water: Journal of Geophysical Research: Solid Earth, v. 91, p. 8151–8176, https://doi.org/10.1029/JB091iB08p08151.

Kohlstedt, D., Keppler, H., and Rubie, D., 1996, Solubility of water in the α, β and γ phases of $(Mg, Fe)_2 SiO_4$: Contributions to Mineralogy and Petrology, v. 123, p. 345–357, https://doi.org/10.1007/s004100050161.

Li, X.P., Rahn, M., and Bucher, K., 2004, Serpentinites of the Zermatt-Saas ophiolite complex and their texture evolution: Journal of Metamorphic Geology, v. 22, p. 159–177, https://doi.org/10.1111/j.1525-1314.2004.00503.x.

Li, X.P., Rahn, M., and Bucher, K., 2008, Eclogite facies metarodingites–phase relations in the system SiO_2-Al_2O_3-Fe_2O_3-FeO-MgO-CaO-CO_2-H_2O: An example from the Zermatt-Saas ophiolite: Journal of Metamorphic Geology, v. 26, p. 347–364, https://doi.org/10.1111/j.1525-1314.2008.00761.x.

Mackwell, S., Kohlstedt, D., and Paterson, M., 1985, The role of water in the deformation of olivine single crystals: Journal of Geophysical Research: Solid Earth, v. 90, B13, p. 11319–11333, https://doi.org/10.1029/JB090iB13p11319.

Mei, S., and Kohlstedt, D., 2000, Influence of water on plastic deformation of olivine aggregates: 1. Diffusion creep regime: Journal of Geophysical Research: Solid Earth, v. 105, p. 21457–21469, https://doi.org/10.1029/2000JB900179.

Mosenfelder, J.L., Deligne, N.I., Asimow, P.D., and Rossman, G.R., 2006, Hydrogen incorporation in olivine from 2–12 GPa: The American Mineralogist, v. 91, p. 285–294, https://doi.org/10.2138/am.2006.1943.

Padrón-Navarta, J.A., Hermann, J., and O'Neill, H.S.C., 2014, Site-specific hydrogen diffusion rates in forsterite: Earth and Planetary Science Letters, v. 392, p. 100–112, https://doi.org/10.1016/j.epsl.2014.01.055.

Padrón-Navarta, J., and Hermann, J., 2017, A subsolidus olivine water solubility equation for the Earth's upper mantle: Journal of Geophysical Research: Solid Earth, v. 122, p. 9862–9880, https://doi.org/10.1002/2017JB014510.

Peacock, S.A., 1990, Fluid processes in subduction zones: Science, v. 248, p. 329–337, https://doi.org/10.1126/science.248.4953.329.

Schmidt, M.W., and Poli, S., 1998, Experimentally based water budgets for dehydrating slabs and consequences for arc magma generation: Earth and Planetary Science Letters, v. 163, p. 361–379, https://doi.org/10.1016/S0012-821X(98)00142-3.

Shen, T., Hermann, J., Zhang, L., Padrón-Navarta, J.A., and Chen, J., 2014, FTIR spectroscopy of Ti-chondrodite, Ti-clinohumite, and olivine in deeply subducted serpentinites and implications for the deep water cycle: Contributions to Mineralogy and Petrology, v. 167, p. 992–1007, https://doi.org/10.1007/s00410-014-0992-8,.

Smyth, J., Frost, D., Nestola, F., Holl, C., and Bromiley, G., 2006, Olivine hydration in the deep upper mantle: Effects of temperature and silica activity: Geophysical Research Letters, v. 33, https://doi.org/10.1029/2006GL026194.

Tielke, J.A., Zimmerman, M.E., and Kohlstedt, D.L., 2017, Hydrolytic weakening in olivine single crystals: Journal of Geophysical Research: Solid Earth, v. 122, p. 3465–3479, https://doi.org/10.1002/2017JB014004.

Walker, A., Hermann, J., Berry, A.J., and O'Neill, H.S.C., 2007, Three water sites in upper mantle olivine and the role of titanium in the water weakening mechanism: Journal of Geophysical Research: Solid Earth, v. 112, https://doi.org/10.1029/2006JB004620.

Wicks, F., and Whittaker, E., 1977, Serpentine textures and serpentinization: Canadian Mineralogist, v. 15, p. 459–488.

Manuscript received 31 January 2018
Revised manuscript received 20 April 2018
Manuscript accepted 24 April 2018

Printed in USA